

STRUCTURAL AND MAGNETIC PROPERTIES OF COPPER FERRITE NANOPARTICLES

C. M. Kale^{#1}, M. K. Babrekar¹, S. D. More², S. J. Shukla²

^{#1}Dept. of Physics, Indraraj Arts, Commerce and Science College, Sillod-Aurangabad

²Deogiri Art, Commerce and Science College, Aurangabad. (M. S.) India

^{#3}corresponding author: cmkale1973@gmail.com

Abstract - The pure cobalt ferrite nanoparticles (CFNPs) have been synthesized, investigated and characterised through structural and magnetic measurements. The samples were synthesized via sol-gel autocombustion technique. The room temperature X-ray diffraction (XRD) pattern confirm the formation of single phase spinel structure of the sample. The lattice constant calculated from XRD used to calculate the bulk density, X-ray density, porosity and hopping length. The particle size obtained from the Scherrer formula and linear intercept method by using Scanning Electron Microscopy (SEM) confirms the nanocrystalline nature. Infrared (IR) shows two main absorption band corresponds to (A) and [B] site in spinel structure. The magnetic properties were measured using magnetic hysteresis (M-H) loop tracer at room temperature and at magnetic field 5 KOe. From M-H curves were the magnetic properties such as saturation magnetization, magnetic moment; squareness ratio and coercivity have been reported.

Keywords- Cobalt ferrite, sol-gel technique X-ray diffraction, particle size, magnetic properties

I. INTRODUCTION

Spinel ferrites is the class of ferrite material have a great attention regarding to their particle size dependent structural, magnetic, chemical, electric, mechanical and thermal properties [1-2]. Cobalt ferrite (CoFe_2O_4) is hard ferrite material because of their excellent chemical stability, mechanical hardness, reasonable saturation magnetization and high magneto-crystalline anisotropy [3]. Hence, CoFe_2O_4 nanoparticles (CFNPs) are being a great interest for a wide range of disciplines, such as biomedicine, magnetic fluids, magnetic energy storage, catalysis [4,5], spintronics [6], drug delivery systems [7], and magnetohyperthermia [8] etc. and in many electronic and magnetic applications. It is important to make a material of desirable microstructure, with a high sintered density, a nano-particle size and a narrow particle size distribution [9]. These magnetic materials are intensively influenced by their starting chemical composition and their microstructure, which are more sensitive to the manufacturing process [10]. Spinel ferrites have the general formula MFe_2O_4 (where M is divalent metal ions such as Co, Ni, Zn, Mg, etc.). Altering the divalent cation type and level content in the ferrites, enable us to obtain a large range of different physical and magnetic properties [11]. The basic uses of these spinel ferrites depend on the intrinsic properties such as Curie temperature, saturation magnetization, coercivity, phase, porosity, particle size, etc. Accordingly efforts have already been made to substitute Co or Fe by metal ions for changing the structural, magnetic and electrical properties in a controlled manner as reported in various literatures. Cobalt ferrite is a magnetic semiconductor, where Fe^{2+} and Co^{2+} ions refer to the n-type and p-type carriers respectively. These carriers are localized and isolated from each other and leading to hoping mechanism of charge transport between metal ions of different valences at crystallographically equivalent lattice points as reported in literature [12].

The present study reports on the synthesis, structural and magnetic properties of CFNPs synthesized at room temperatures. We succeeded in preparing the high-quality pure CFNPs around 33 nm by sol-gel autocombustion method which may open new window in the various applications.

II. EXPERIMENTAL

The ultrafine CFNPs sample was prepared by using sol-gel auto combustion method. The starting samples were taken in the form of high purity A. R. grade (>99%) for the preparation of ferrite nitrates as, cobalt nitrate-Co $(\text{NO}_3)_2 \cdot 5\text{H}_2\text{O}$, and ferric nitrate-Fe $(\text{NO}_3)_3 \cdot 9\text{H}_2\text{O}$ all from s.d.fine-chem limited. The citric acid is used as a fuel to increase the rate of reaction is taken in the molar ratio 1:3 i.e. metal nitrates to citric acid. The metal nitrates were dissolved together in a minimum amount of double distilled water to get a clear solution. An aqueous solution of citric acid was mixed with metal nitrates solution, and add ammonia solution was slowly to maintain the pH at 7. The mixed solution was kept on to a hot plate and the solution is continuous stirred at 90°C . During evaporation, the solution became viscous and finally formed a very viscous blackish-brown gel. When all water molecules were removed from the mixture, the viscous gel began frothing. After few minutes, the gel automatically ignited and burnt with glowing flints. The decomposition reaction would not stop before the whole citrate complex was consumed. The auto-ignition was completed within a minute, yielding the black-colored ashes termed as a precursor. The obtained powder was then subjected to further heating treatment into a muffle furnace at relatively low temperature 400°C for 6 h. The final product is then grinded and subjected to further study.

The structural parameters were determined and confirmed by the XRD technique. The CFNPs sample targeted with Cu-K α (wavelength, $\lambda = 1.5406 \text{ \AA}$) to confirm the single phase nature and nano-phase formation of CFNPs at room temperature. The particle size was calculated with the help of XRD pattern by using Scherrer formula, and also by SEM image. The infrared (IR) absorption spectra of all samples were recorded using IR spectrometer in the wave number range $700\text{-}300 \text{ cm}^{-1}$ explain formation of two absorption band and site preference of the metal ions. The magnetic properties measurement were carried out using high field M-H loops tracer recorded at 300K and 5KOe to reach saturation values.

III. RESULTS AND DISCUSSION

3.1. Structural analysis

The XRD technique is used to determine interplanar distances and lattice constant. The room temperature XRD pattern of pure cobalt ferrite is shown in **Fig. 1**.

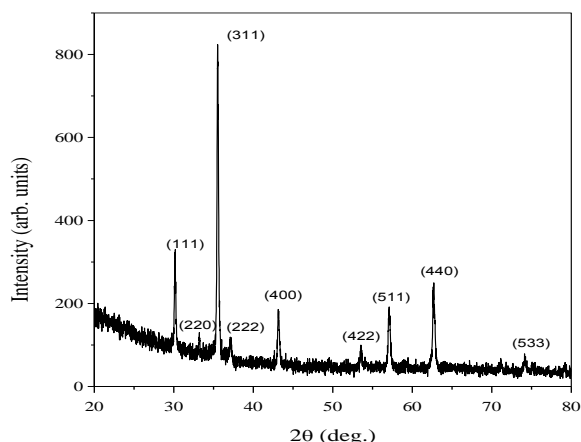


Fig.1: The XRD patterns of CoFe₂O₄ nanoferrite.

In **Fig. 1**; all the peaks shows the sharp, clear Bragg’s peaks that appear in the diffraction patterns can be identified with the help of JCPDS data and from XRD, Bragg’s peaks confirms the formation of single-phase cubic spinel structure as the corresponding planes such as (220), (311), (222), (400), (422), (511), and (440) are indexed by miller indices [hkl]. The strongest reflection comes from (311) plane that indicates spinel phase and the existence of broad peaks in the XRD patterns indicates the fine particle nature in nanosize dimensions of the prepared ferrite [13]. There are no any extra peaks observed means there is absence of any other impurity phase. All the peaks are reveals that the entire samples possess the single phase cubic spinel structure. Using XRD data, the lattice constant (a) calculated by using the following relation,

$$a = d\sqrt{h^2 + k^2 + l^2} \text{ \AA}$$

where, all symbols carry their usual meanings. The calculated lattice constant is good agreement with the standard. The average particle size (t in Å) calculated from full width at half maximum (FWHM) the broadening of most intense peaks (311) using the classical Debye-Scherrer formula [14]. The values of particle size obtained from XRD data and SEM are given in **Table 1**. The average particle size is found ~33nm which are close to the results obtained from SEM images and good agreement with report of Sonal Singhal et.al. [15]

TABLE I
STRUCTURAL PARAMETER OF COBALT FERRITE

Structural Parameter		Value
Chemical formula		CoFe ₂ O ₄
Lattice constant	(a)	8.3652 Å
X-ray density dx	dx	5.324 g/cm ³
The bulk density	d	3.523 g/cm ³
Percentage porosity	% P	33.83
Hopping length	L _A	3.6221 Å
	L _B	2.9579 Å
Particle size	XRD	33.27 nm
	SEM	33 nm
Absorption band frequency	ν ₁	546.54 cm ⁻¹
	ν ₂	448.33cm ⁻¹

The bulk density (d), X-ray density (dx), the percentage porosity (% P) is listed in **Table 1**. The X-ray density is attributed to the facts it depends on the atomic weight of Co (58.93). The high values of porosity suggest that the prepared sample becomes porous with and such types of material are generally used for sensors and coating technology. Bond lengths R_A and R_B are the shortest distance between A-site and B-site cations with the oxygen ion respectively. The calculated by using the equation [16] and values are listed in **Table 1**. The values R_B are greater than R_A indicates that the B-site cations Co²⁺ are closer to oxygen O²⁻ ions exerts more attractive force. The hopping length ‘L_A’ and ‘L_B’ is calculated from the following equations [17] L_A = 0.25 a√3 Å and L_B = 0.25a√2 Å

From the values given **Table 1** indicates that, L_A (3.6221 Å) is larger than L_B (2.9579 Å) means the jump lengths of magnetic ions in the tetrahedral A-site is more that octahedral B-site.

3.2. Infrared analysis

Infrared (IR) spectroscopic technique is used as a fingerprints obtained in a transmittance (%) of the IR radiation plotted against wavenumber. In ferrites the metal ions are situated in two different sublattices designated tetrahedral (A) site and octahedral [B] site, according to the geometrical configuration of the oxygen nearest neighbours have attributed the band around 600 cm^{-1} and 400 cm^{-1} . In the present investigation the absorption spectra shows two major absorption bands i.e. higher absorption band (ν_1) lies in the range of 546.54 cm^{-1} and lower absorption band (ν_2) in the range 448.33 are assigned to the tetrahedral (A) and octahedral [B] sites shown in **Fig.2**. The values of absorption bands (ν_1 and ν_2) are presented in **Table 1** shows that ν_1 goes on increasing while ν_2 decreases. The difference in frequencies of ν_1 and ν_2 is due to changes in the bond length $\text{Fe}^{3+}\text{-O}^{2-}$ at tetrahedral and octahedral sites. The remaining bands are probably due to combinational frequencies or overtones. The nature of absorption bands in the infrared spectra depends on the distribution and type of cations among octahedral and tetrahedral sites [18].

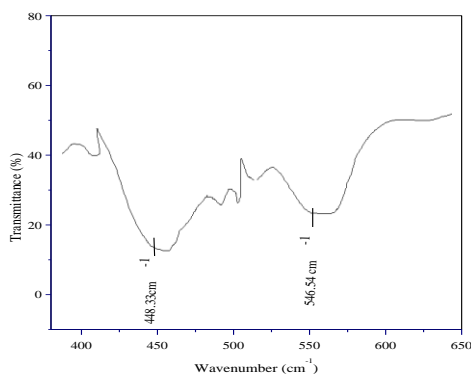


Fig.2: The IR spectra of CoFe_2O_4 nanoferrite.

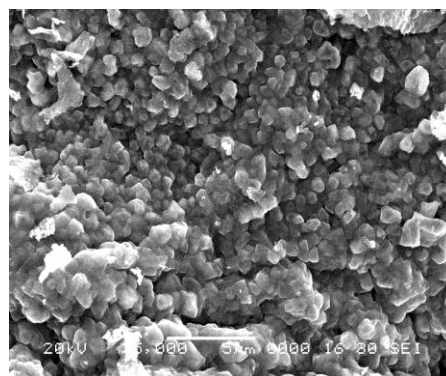


Fig.3: The SEM micrograph cobalt ferrite material

3.3. Scanning Electron Morphology

The scanning electron microscopy (SEM) is one of the powerful techniques used to analyze the microstructure of ferrites. The SEM micrograph cobalt ferrite material is shown in **Fig.3**. The particle size was also determined from SEM images by linear intercept method. The morphology of particle is almost uniform shape, its size 33 nm is calculated and given in **Table 1**. It is evident from SEM images that the prepared samples are porous in nature. Small amount of pores in SEM images reveals that the sintering is done in a satisfactory manner.

3.4. Magnetic properties analysis

The M-H plots helps to understand the magnetic response of material and provides the information about the magnetic properties such as saturation magnetization (M_s), coercivity (H_c), remanence magnetization (M_r) etc. All the measurements were carried out at room temperature 300K and magnetic field 5KOe . The hysteresis loop of Cobalt ferrite is depicted in **Fig.4** and magnetic parameters are given in **Table 2**.

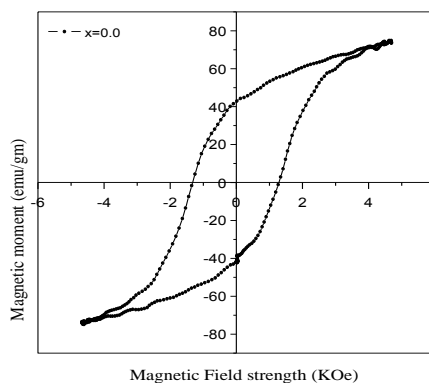


Fig.4: Magnetic hysteresis (M-H) plots for the CoFe_2O_4 ferrite

TABLE II
MAGNETIC PARAMETER OF COBALT FERRITE

Magnetic Parameter	Values
M_s	74.86 (emu/gm)
M_r	76.22 (emu/gm)
SQR ratio	1.018
H_c	1304.3(Oe)
nB	3.14(μB)

The M_s Values obtained from the steady part of graph at which no change in magnetisation as magnetic field increases. It is observed that M_s value of the prepared sample is 74.86 emu/g. The intensity of the magnetic field required to reduce the magnetisation of the samples to zero, after the magnetisation of the sample has reached saturation. The results obtained agree well with the published literature of J. Wang et.al. [18].

The saturation magnetization shows less value than remanence magnetization and the remanence magnetization values show that the prepared samples are of nano crystalline nature.

The values of squareness ratio (SQR) of the prepared samples are obtained from M-H plots provide the useful information regarding the domain state of the samples from the ratio of remanence magnetization (M_r) to saturation magnetization (M_s). It is observed from **Table 2**; the SQR almost decreases from 1.018. The large SQR values are useful in many applications such as recording media, magnetic tape etc. The coercivity denoted here as H_c , also called coercive force and used as the most important single criterion for determining whether a ferromagnetic material is soft (low value of H_c) or hard (high value of H_c). Keeping coercivity value at minimum scale is a primary goal in the preparation of magnetic material. In this study, the coercivity of the CFNPs is 1304.3 indicates that the prepared samples possess nanocrystalline nature. Our experimental results are fairly agreed with the other nanocrystalline spinel ferrite. The magneton number n_B of the sample was calculated using the known values of molecular weight and saturation magnetization at room temperature is found 3.14 listed in **Table 2**.

IV. CONCLUSIONS

To structural and magnetic properties of cobalt ferrite system were successfully synthesized by sol-gel auto combustion technique. The XRD spectra show the formation of cubic spinel structure. The particle size calculated by the Sherrer formula is 33 nm and the value of lattice constant is agreed with the reported value in the literature. The hopping length L_A and L_B varies with respect to lattice constant. IR analysis shows two absorption bands at $\sim 600 \text{ cm}^{-1}$ and 400 cm^{-1} depends on the distribution and type of cations among octahedral and tetrahedral sites. SEM study reveals that the particle size of all the samples is in nanometer dimension. Saturation magnetization, remanence field, SQR, coercivity and magneton number, explains the magnetic properties of the Co ferrite.

ACKNOWLEDGMENT

The author (CMK) is thankful to Professor K. M. Jadhav, Department of Physics, Dr. Babasaheb Ambedkar Marathwada University, Aurangabad (M.S.) India; for his support and fruitful discussion.

REFERENCES

- [1]. Y. Z. Donga, S. H. Piao, K. Zhang, H. J. Choi, *Colloids and Surfaces A* **537**, 102 (2018).
- [2]. J. Dong, Y. Zhang, X. Zhang, Q. Liu, J. Wang, *Materials Letters* **120**, 9 (2014).
- [3]. Waje SB, Hashim M, Ismail I. *J Magn Magn Mater.* 2011;323(11):1433-9.
- [4]. Issa B, Obadia IM, Albas BA, Haik Y (2013) *Int J Mol Sci* 14:21266-21305.
- [5]. Chomoucka J, Drbohlovova J, Huska D, Adam V, Kizek R, et al. (2010) *62*: 144-149.
- [6]. U. Luders, A. Barthelemy, M. Bibes, K. Bouzehouane, S. Fusil, E. Jacquet, J. P. Contour, J. F. Bobo, J. Fontcuberta, and Fert, *Advanced Materials* **18**, 1733 (2006).
- [7]. H. Gu, K. Xu, Z. Yang, C. K. Chang, and B. Xu, *Chemical Communications* **34**, 4270 (2005).
- [8]. G. Baldi, D. Bonacchi, C. Innocenti, G. Lorenzi, and C. Sangregorio, *Journal of Magnetism and Magnetic Materials* **311**, 10 (2007).
- [9]. Ahn Y, Choi EJ, Kim S, Ok HN (2001). *Mater Lett* 50:47-52.
- [10]. Dong S. X., Li JF, Viehland D. *Appl Phys Lett* 84,(2004), 4188-4191
- [11]. C. M. Kale, P. P. Bardapurkar, S. J. Shukla, K. M. Jadhav, *J. Magn. Magn. Mater.* 331 (2013) 220-224
- [12]. P. C. Kau, T. S. Tsai, *J. Appl. Phys.* 65 (1989) 4349
- [13]. Hankare P. P., Patil R. P., Sankpal U. B., Jadhav S. D., Mulla I. S., Jadhav K. M., Chougule B. K. *J. Magn. Mag. Mater.* 321, 19(2009).
- [14]. Cullity B. D., Stock S. R., *Elements of X-ray diffraction* (New York, Prentice Hall) (2001) 154
- [15]. Sonal Singhal, Sheenu Jauhar, Kailas Chandra, Sandeep Bansal. *Bull. Mater. Sci.* Vol.36 No.1, 107-114 (2013).
- [16]. Standley K. J., *Oxide Magnetic Material*, Oxford, U. K. Clarendon (1972)
- [17]. R. H. Kadam, S. S. More, A. B. Kadam, D. R. Mane, G. K. Bichile, *Open Chem.* 8 (2010) 419.
- [18]. J. Wang, Q. Chen, S. Che, *J. Magn. Magn. Mater.* 280 (2004) 281